

# Fermi Edge Singularities: Bound-states and Finite Size Effects

Alexandre M. Zagoskin<sup>1</sup> and Ian Affleck<sup>1,2</sup>

<sup>1</sup>*Department of Physics and Astronomy and* <sup>2</sup>*Canadian Institute for Advanced Research, The University of British Columbia, Vancouver, B.C., V6T 1Z1, Canada*

Fermi edge adsorption singularities (FES) are studied using a combination of conformal field theory (CFT), an exact sum rule and numerical work on a tight binding model which is shown to exhibit remarkable simplifying features. The relationship between FES and the Anderson orthogonality exponent is established in great generality, using CFT, including the case where the core hole potential produces a boundstate. Universal results on the adsorption intensity in a finite sized sample are obtained. Various predictions are checked numerically and the evolution of the adsorption intensity with electron density is studied.

## I. INTRODUCTION

A theoretical understanding of the Fermi edge singularity (FES) in X-ray adsorption in metals and of the related Anderson orthogonality catastrophe dates back to the 1960's.<sup>1,2,3,4,5,6,7,8,9,10</sup> Nonetheless, this remains an active area of research today, in part because of theoretical and experimental work in systems of reduced dimensionality where strong correlation effects may play an important role.<sup>11,12,13,14,15,16,17,18</sup> In particular a new and very general theoretical approach has been developed, based on conformal field theory.<sup>12</sup>

Recent experiments have studied optical absorption threshold singularities in modulated, doped semi-conductor layered structures.<sup>17,18</sup> These behave more or less like two dimensional metals with a continuously tunable electron density. The potential produced by the valence band hole is expected to produce a boundstate (exciton) due to the well-known theorem that an attractive potential in two dimensions always has a boundstate. Many interesting issues are raised by these experiments which have not yet been adequately addressed theoretically. In particular, it is possible to study the behaviour of the threshold singularities as the electron density goes to 0. In some cases an additional threshold corresponding to a negatively charged exciton (two conduction electrons bound to a valence hole) is observed. Strong correlation effects may play a crucial role in this case and the usual Fermi liquid approach may need to be modified.

The present work addresses several issues in this field, within the usual Fermi liquid framework. The case of a core potential producing a boundstate is considered, as is the behaviour of the threshold singularities as a function of electron density. Furthermore, we consider the nature of the adsorption intensity for a simple model of a finite sample. The techniques employed in this paper are a combination of conformal field theory methods, an exact sum rule and numerical work on a tight binding model which exhibits remarkable simplifying features making it feasible to study very large systems.

The conformal field theory method of Ref. ( 12) is extended to the case where there is a boundstate. A very simple and general proof of the exact correspondence between the FES exponent and the orthogonality exponent is given. The adsorption intensity near threshold, for a finite system is shown to have a simple universal form, using conformal field theory. An exact sum rule is introduced which determines the ratio of adsorption intensities for the two cases where the core bound state is empty or filled.

Numerical work on the simple tight binding model is used to check the validity of Anderson's formula relating the orthogonality exponent to the phase shift at the Fermi surface, the Nozières-de Dominicis, Combescot-Nozières formulas<sup>2,6</sup> for FES exponents including the boundstate case, and the formulas newly derived here for the adsorption intensity in a finite system. In addition this numerical work, together with the sum rule, is used to study the behaviour of the adoption intensity as a function of density.

Some of the new conformal field theory results were briefly described in Ref. ( 19).

## II. CONFORMAL FIELD THEORY APPROACH

An approach based on boundary conformal field theory<sup>12,19</sup> provides a unified view of the problem. As usually, we start from the simplest possible model<sup>2</sup>,

$$\mathcal{H} = \sum_{\mathbf{k}} \epsilon_{\mathbf{k}} c_{\mathbf{k}}^{\dagger} c_{\mathbf{k}} + b^{\dagger} b \sum_{\mathbf{k}, \mathbf{k}'} V_{\mathbf{k}, \mathbf{k}'} c_{\mathbf{k}}^{\dagger} c_{\mathbf{k}'} + E_0 b^{\dagger} b. \quad (2.1)$$

Here the band of spinless, non-interacting electrons ( $c^{\dagger}, c$ ) is scattered by the core hole potential  $V_{\mathbf{k}, \mathbf{k}'}$ . The core hole ( $b^{\dagger}, b$ ) is dispersion-less. It is created and annihilated instantaneously (by irradiation), and the reaction of the band electrons on this instantaneous perturbation constitutes the FES and Anderson orthogonality effects.

In the low-energy limit, the system is mapped onto the (1+1)-dimensional Dirac Fermions defined on a ray  $r > 0$  with a scattering potential  $V$  at the origin. (This can be done by assuming spherical symmetry of  $\epsilon_{\mathbf{k}}$  and  $V_{\mathbf{k}, \mathbf{k}'}$  and considering only s-wave scattering; generalizations to other cases are straightforward.) The following discussion applies, with minor modifications, to either an s-wave projected 3D (3 dimensional) problem or to a problem defined a priori in 1D. We will henceforth generally consider the 1D case. We could consider, for example, a 1D tight-binding model, defined on the positive half-line, with free boundary conditions and a potential localized near  $x = 0$ . See Appendix A for a detailed discussion of this model. The corresponding boundary condition in the low energy Dirac theory is:

$$\psi_L(0) = \psi_R(0). \quad (2.2)$$

The role of the scattering potential in the theory here is to impose an effective boundary condition on the low energy degrees of freedom, relating the left and right movers:

$$\psi_R(0) = e^{2i\delta(k_F)} \psi_L(0), \quad (2.3)$$

Here  $\delta(k_F)$  is the phase shift at the Fermi surface;  $k$ -dependence of the actual phase shift is irrelevant at low energies. The action of the hole creation operator,  $b^{\dagger}$ , thus reduces to that of a primary boundary condition changing operator,  $\mathcal{O}$ . The Green's function (hole propagator) of this operator in a half-plane,  $z = r + i\tau, r \geq 0$ , is

$$G(\tau_1 - \tau_2) \equiv \langle b(\tau_1) b^{\dagger}(\tau_2) \rangle = \langle A; 0 | \mathcal{O}(\tau_1) \mathcal{O}(\tau_2) | A; 0 \rangle = \frac{1}{(\tau_1 - \tau_2)^{2x}}. \quad (2.4)$$

Here  $x$  is the scaling dimension of  $\mathcal{O}$ , and  $|A; 0\rangle$  is the ground state of the infinite system (filled Fermi sea) without scattering potential. Physically, the Green's function is directly related to the absorption intensity in the case of photoemission,

$$I(\omega) \propto \int dt e^{i(\omega - \omega_0)t} \langle b(t) b^{\dagger}(0) \rangle \propto (\omega - \omega_0)^{-\alpha}, \quad (2.5)$$

where  $\omega_0$  is the threshold frequency. Evidently, the (FES-) exponent  $\alpha$  and the scaling dimension are related via

$$\gamma \equiv 1 - \alpha = 2x. \quad (2.6)$$

Looking for finite size effects, we conformally map the half-plane onto the strip,  $l \geq r \geq 0$  Using the transformation  $z = l e^{\pi w/l}$ . In a bosonic system this automatically gives the same boundary condition at 0 and  $l$ . However, for fermions it gives:

$$\psi_L(0) = \psi_R(0), \quad \psi_L(l) = -\psi_R(l). \quad (2.7)$$

This follows because the fermion fields transform as:

$$\begin{aligned} \psi_L &\rightarrow (dz/dw)^{1/2} \psi_L \\ \psi_R &\rightarrow (dz^*/dw^*)^{1/2} \psi_R. \end{aligned} \quad (2.8)$$

At  $w = x + il$ ,

$$(dz/dw)^{1/2} / (dz^*/dw^*)^{1/2} = -1. \quad (2.9)$$

This transformed problem corresponds to considering a 1D model defined on a finite line,  $0 < x < l$ , with the impurity potential near  $x = 0$  and an appropriate boundary condition at  $x = l$ . Alternatively, the 3D s-wave projected system is now defined inside a finite sphere of radius  $l$  with an appropriate boundary condition on the surface of the sphere. For a discussion of this boundary condition and more details, see Appendix A.

We find for the Green's function on the strip

$$\langle AA; 0 | \mathcal{O}(u_1) \mathcal{O}(u_2) | AA; 0 \rangle = \frac{1}{\left(\frac{2l}{\pi} \sinh \frac{\pi}{2l}(u_1 - u_2)\right)^{2x}}, \quad (2.10)$$

$|AA; 0\rangle$  being the unperturbed ground state of the system of length  $l$ , with the “same” boundary condition,  $A$ , given by Eq. (2.3) at both ends.

In Eq. (2.10) we can either Taylor expand  $\sinh$  in the limit  $\pi(u_1 - u_2)/l \ll 1$ , or insert a complete set of states  $|AB; m\rangle$  (eigenstates of the system with the scattering potential - boundary condition “B” - present), and obtain the relation

$$\begin{aligned} & \left(\frac{\pi}{l}\right)^{2x} e^{-\frac{\pi x(u_1 - u_2)}{l}} \left(1 + 2xe^{-\frac{\pi(u_1 - u_2)}{l}} + \frac{2x(2x+1)}{2} e^{-\frac{2\pi(u_1 - u_2)}{l}} \right. \\ & \left. + \frac{2x(2x+1)(2x+2)}{6} e^{-\frac{3\pi(u_1 - u_2)}{l}} + \dots\right) = \sum_m |\langle AA; 0 | \mathcal{O} | AB; m \rangle|^2 e^{-[E_m^{AB} - E_0^{AA}][u_1 - u_2]}. \end{aligned} \quad (2.11)$$

If for the operator  $\mathcal{O}$  the first nonvanishing matrix element is with the ground state of the perturbed system,  $|AB; 0\rangle$ , then for the overlap of the two ground states (Anderson orthogonality catastrophe)

$$|\langle AA; 0 | \mathcal{O} | AB; 0 \rangle| = \left(\frac{\pi}{l}\right)^x. \quad (2.12)$$

The Anderson orthogonality exponent coincides with the scaling dimension  $x$ ; on the other hand,  $x$  is given by the  $O(1/l)$ - contribution to the ground state energy shift due to the perturbation,<sup>12,19</sup>

$$x = \frac{l}{\pi} [E_0^{AB} - E_0^{AA}]. \quad (2.13)$$

Here it is being implicitly assumed that this energy difference consists of a term of  $O(1/l)$  only, as would follow from conformal invariance. As discussed in Appendix A there will in general also be a term of  $O(1)$  which must be subtracted.

A simple way of determining the Fermi edge exponent  $\gamma$  and the orthogonality exponent  $x$ , is thus to calculate the  $1/l$  finite-size correction to the difference in groundstate energies of the system with and without the scattering potential. The term of  $O(1)$  is non-universal, (cut-off dependent) while the higher order terms contain the corrections from various irrelevant operators. On the other hand, we expect the term of  $O(1/l)$ , which is determined only by the immediate vicinity of the Fermi surface, to be universal and to give the desired FES and orthogonality exponents. In fact, this result remains true including bulk Coulomb interactions in one dimension.<sup>12</sup> Thus calculation of the  $O(1/l)$  term in the groundstate energy difference gives a very simple way of determining the FES and orthogonality exponents in great generality. This calculation is spelled out in detail, for a one-dimensional tight-binding model, in App. A. The conclusion is:

$$x = \frac{1}{2} \left[ \frac{\delta(k_F)}{\pi} \right]^2. \quad (2.14)$$

While various derivations of this result, both for the FES exponent and for the orthogonality exponent have been given before, this one has certain distinct advantages. The original derivation of the orthogonality exponent by Anderson made a variety of approximations, including Taylor expanding certain quantities in powers of the phase shift. The derivation of the FES exponent in[ 2] also initially assumed a small  $\delta(k_F)$  and then argued for the generality of the result by some fairly subtle consistency arguments. The bosonization derivations start with a bosonized Hamiltonian written in terms of  $\delta(k_F)$  whereas a naive bosonization in fact only picks up the Born approximation to  $\delta$ , linear in the scattering potential. It is expected that eliminating the high energy modes somehow renormalizes this parameter in the bosonized Hamiltonian, turning it into the true phase shift. Once the assumption of conformal invariance is made, it is very straightforward to demonstrate that it is precisely the phase shift at the Fermi surface which enters the exponents, by an explicit calculation of the groundstate energy, as given in App. A. We note that once the bosonized Hamiltonian is assumed, the results for the strip can be obtained by a mode expansion of the boson field. This, of course, gives the same result obtained more simply by the conformal transformation.

Another advantage of this somewhat abstract approach to the problem is that it can be immediately generalized to the case where the core potential creates a boundstate. The Green’s function can then be presented as a sum of two terms:

$$\begin{aligned}
G(u) = G_e(u) + G_f(u) = & \sum_m |\langle AA; 0 | \mathcal{O} | AB; m; e \rangle|^2 e^{-[E_{m,e}^{AB} - E_0^{AA}]u} \\
& + \sum_n |\langle AA; 0 | \mathcal{O} | AB; n; f \rangle|^2 e^{-[E_{n,f}^{AB} - E_0^{AA}]u},
\end{aligned} \tag{2.15}$$

where the first sum is taken over all states  $|AB; m; e\rangle$  where the boundstate is empty, and the second over the states  $|AB; n; f\rangle$  where it is filled. These two terms give rise to two peaks in the absorption rate, separated by the binding energy,  $\Delta\omega = |E_B|$ . Introducing the occupation number of the boundstate,  $\hat{n}_B$ ,

$$G(u) = \langle [b(u)\hat{n}_B(u)][\hat{n}_B(0)b^\dagger(0)] \rangle + \langle [b(u)(1 - \hat{n}_B(u))][\hat{n}_B(0)b^\dagger(0)] \rangle. \tag{2.16}$$

In the long time limit we may calculate each of these terms separately using the boundary conformal field theory approach. The boundstate is associated with a finite binding energy,  $E_B$  and an exponentially decaying wave-function. Thus it has no direct effect on the  $O(1/l)$  terms in the energies. Therefore we expect the above formulas to apply immediately for the first threshold where the boundstate is filled, with the exponent:

$$x_f = \frac{1}{2} \left[ \frac{\delta(\epsilon_F)}{\pi} \right]^2. \tag{2.17}$$

When the boundstate is empty, the only change in the low energy physics is that one additional electron is raised to the first unoccupied state above the Fermi surface. This has wave-vector:

$$k = k_F + \frac{\pi}{l} \left[ \frac{1}{2} - \delta(\epsilon_F) \right]. \tag{2.18}$$

We may regard  $b[1 - n_B]$  as a different boundary condition changing operator which creates one additional low energy electron, in addition to producing the new boundary condition of Eq. (2.3). The  $O(1/l)$  term in the ‘‘groundstate’’ energy difference in the case of the empty boundstate is, from App. A:

$$E'_0 - E_0 = v_F \frac{\pi}{l} \frac{1}{2} \left[ \frac{\delta(\epsilon_F)}{\pi} - 1 \right]^2 \tag{2.19}$$

Thus the orthogonality exponent giving the overlap between the unperturbed groundstate and the ‘‘groundstate’’ with the boundstate empty is:

$$x_e = \frac{1}{2} \left[ \frac{\delta(\epsilon_F)}{\pi} - 1 \right]^2. \tag{2.20}$$

The FES exponents for the two thresholds  $\alpha_f$  and  $\alpha_e$  are given by:

$$\alpha_f = 1 - 2x_f, \quad \alpha_e = 1 - 2x_e. \tag{2.21}$$

By merely computing the groundstate energy, rather than attempting to compute the exponents directly, we have finessed the problem of attempting to bosonize the theory with the boundstate. We note that these results agree with Combescot and Nozières<sup>6</sup> and Hopfield<sup>4</sup>. The present derivation seems quite closely related to the observation of Hopfield that the FES exponent measures the amount of charge pulled in from infinity by the boundstate.

The conformal mapping from the plane to the strip establishes in a simple way the relationship between the FES exponents of the infinite system and the orthogonality exponents and energies of the finite system. In fact this mapping provides considerably more information. Let’s imagine a rather artificial situation where a core hole is instantaneously created at the end of a finite one-dimensional system. (Equivalently we could consider an artificial situation where it is created at the centre of a finite sphere.) In this case the adsorption intensity,  $I(\omega)$  of Eq. (2.5) becomes a series of  $\delta$ -function peaks, as we see from Fourier transforming Eq. (2.11). The peaks occur at  $\omega_m = E_m^{AB} - E_0^{AA} = \pi(x+m)/l$ , the energies of excited states of the perturbed system measured from the unperturbed ground state energy  $E_0^{AA}$ . [The neglected term of  $O(1)$  just shifts the threshold by  $\omega_0$ .] It follows from (2.11) that the ratio of the  $m$ th peak to the zeroth one depends only on  $x$ :

$$\frac{|\langle AA; 0 | \mathcal{O} | AB; m \rangle|^2}{|\langle AA; 0 | \mathcal{O} | AB; 0 \rangle|^2} = \frac{2x(2x+1)(2x+2)\dots(2x+m-1)}{m!}. \tag{2.22}$$

Note that, from Eq. (2.11), each of these peak intensities scales with length the same way as does the 0<sup>th</sup> peak, considered by Anderson, given by Eq. (2.12). The ratios of peak intensities are length independent pure universal numbers, determined only by  $\delta(k_F)$ .

In fact, each of these peaks corresponds, in general, to several different states with energies that are degenerate, to  $O(1/l)$ . These are simply multiple particle-hole excitations of the free fermion system, with a dispersion relation which is linearized and a phase shift which is assumed  $k$ -independent, near the Fermi surface. A general particle-hole excitation may be constructed by first raising  $n_m$  electrons  $m$  levels, then raising  $n_{m-1}$  electrons  $m-1$  levels, etc. The energy relative to the groundstate of this state is:

$$E_m^{AB} - E_0^{AB} = \frac{\pi}{l} \sum_{p=1}^{\infty} n_p p. \quad (2.23)$$

The first excited state has  $n_1 = 1$ ,  $n_p = 0$  for  $p > 1$ . The next degenerate pair of states have  $n_1 = 2$  or  $n_2 = 1$  (with the other  $n_p = 0$ ). The third set of excited states is threefold degenerate with  $n_1 = 3$  or  $n_1 = n_2 = 1$  or  $n_3 = 1$  (and the other  $n_p = 0$  in all cases). Corrections to the linear dispersion relation and variation of  $\delta(k)$  near  $k_F$  will split these energies by amounts of  $O(1/l^2)$ . The simple prediction obtained here from a conformal transformation does not give the amplitude of each peak separately, but only the sum of amplitudes of all peaks at a given energy, where energy differences of  $O(1/l^2)$  are ignored.

This new finite size result interpolates, in a sense, between the orthogonality exponent and the FES exponent. Considering the large  $m$  limit of Eq. (2.22) we find that the intensity decays as  $m^{-(1-2x)}$ , recovering the FES exponent.

This result applies immediately to the peaks corresponding to the boundstate being filled or empty, provided that the appropriate orthogonality exponents,  $x_f$  and  $x_e$  of Eq. (2.17) and (2.20) are used.

### III. ONE-DIMENSIONAL TIGHT-BINDING MODEL

An evident discrete counterpart to the system (2.1) in its one-dimensional version is the system of spinless fermions on a finite 1D chain with nearest-neighbour hopping, free boundary conditions and an impurity potential which can be switched on/off at the first site:

$$\begin{aligned} \mathcal{H} &= H_0 + b^\dagger b H_1; \\ H_0 &= -t \sum_{i=1}^{l-2} (\psi_i^\dagger \psi_{i+1} + \psi_{i+1}^\dagger \psi_i); \\ H_1 &= -V \psi_1^\dagger \psi_1. \end{aligned} \quad (3.1)$$

Here we choose  $V$  to be positive in case of an attractive core potential, and also choose  $t > 0$ . This model is very amenable to large scale numerical work with a minimum of effort. Not only can the single particle energies and wave-functions for finite  $l$  be found exactly in a simple form, but, more remarkably, the overlaps of the single particle wave-functions corresponding to different values of the potential,  $V$ , obey an exact factorization. This enormously simplifies the calculation of the overlap of the many-particle, Bloch determinant, wavefunctions. This can then be expressed by the Cauchy determinant formula, used as an approximation by Anderson in his classic paper on the orthogonality catastrophe.<sup>10</sup> The many-body overlaps are easily evaluated numerically and in some limits analytically (e.g. in the narrow band limit,  $\frac{t}{V} \rightarrow 0$ ). As a result, chains of length up to few thousand sites are easily handled on a workstation using the standard ‘‘Mathematica’’ package. The crucial factorizability of one-particle overlaps disappears under any other position of the scattering potential.

The details are given in the Appendix B; here we just summarize a few salient features, beginning with the infinite  $l$  limit. This model has a band of eigenstates with exact wave-functions:

$$\Psi_j \propto \sin[kj + \delta(k)], \quad j = 1, 2, 3, \dots \quad (3.2)$$

The dispersion relation is:

$$\epsilon(k) = -2t \cos k. \quad (3.3)$$

The phase shift is given by:

$$\delta = \arctan \left[ \frac{\sin k}{t/V - \cos k} \right]. \quad (3.4)$$

Note that at the bottom of the band,  $k \rightarrow 0$ ,  $\delta \rightarrow 0$  for  $V < t$ , when there is no boundstate, but  $\delta \rightarrow \pi$ , for  $V > t$  when there is a boundstate, as required by Levinson's theorem. As  $k$  ranges over the whole band, from 0 to  $\pi$ ,  $0 \leq \delta(k) \leq \pi/2$  for  $V < t$ , and  $0 \leq \delta(k) \leq \pi$  for  $V > t$ , as shown in Fig. (1). For  $V \gg t$ ,  $\delta(k) \approx \pi - k$ . There is one boundstate, if  $V > t$  only, with:

$$E_B = -(V + t^2/V). \quad (3.5)$$

Note that this approaches the bottom of the band,  $-2t$ , as  $V \rightarrow t$ , where the boundstate disappears.

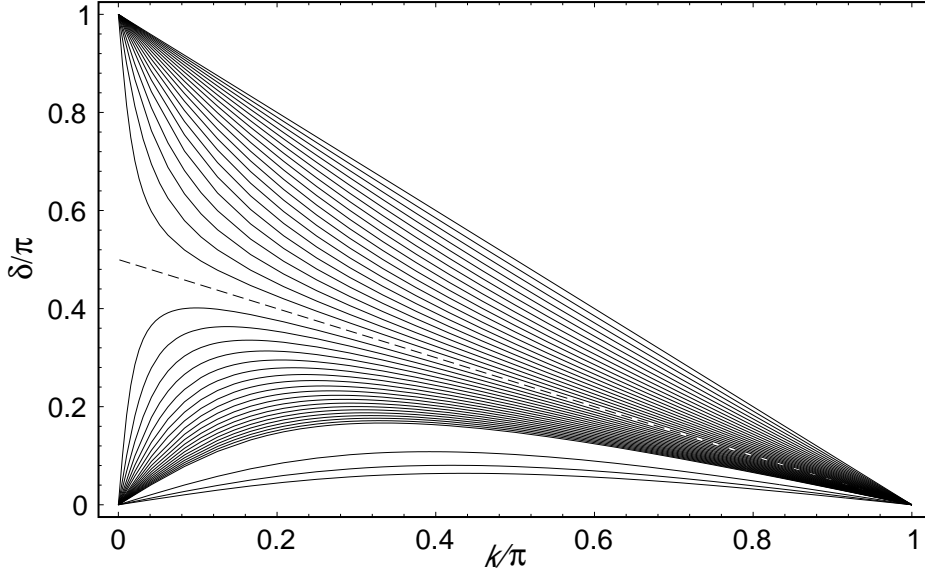


FIG. 1. Phase shift in the 1D tight-binding model vs. density  $\nu = \lim_{l \rightarrow \infty} N/(l-1)$ , at  $t/V = 0, 0.05, 0.01, \dots, 2, 3, 4, 5$ . The dotted line  $t/V = 1$  separates regions with and without boundstate.

The exact boundstate wavefunction is:

$$\Psi_j^B \propto e^{-\kappa j}, \quad (3.6)$$

with

$$\kappa = \ln(V/t). \quad (3.7)$$

For finite  $l$ , there is a set of wavefunctions:

$$\Psi_j^n \propto \sin \tilde{k}_n(j-l), \quad (3.8)$$

with the allowed wave-vectors determined by:

$$\frac{\sin k(l-1)}{\sin kl} = \frac{t}{V}. \quad (3.9)$$

For  $t/V > 1 - 1/l$  there are  $l-1$  solutions of Eq. (3.9), which we label

$$\tilde{k}_1, \tilde{k}_2, \dots, \tilde{k}_{l-1}. \quad (3.10)$$

For  $t/V < 1 - 1/l$  there are only  $l-2$  such wavefunctions, which we label  $2, 3, \dots, (l-1)$  and an additional wavefunction:

$$\tilde{\Psi}_j^1 \propto \sinh \kappa(j-l), \quad (3.11)$$

with  $\kappa$  the solution of:

$$\frac{\sinh \kappa(l-1)}{\sinh \kappa l} = \frac{t}{V}. \quad (3.12)$$

In the case  $V = 0$ , the wave-vectors are:

$$k_n = \pi n/l, \quad n = 1, 2, 3, \dots (l-1). \quad (3.13)$$

From Eq. (3.9) we see that, in the limit  $V/t \rightarrow \infty$ , the wave-vectors are:

$$\tilde{k}_n = (n-1)\pi/(l-1), \quad n = 2, 3, 4, \dots (l-1), \quad (3.14)$$

corresponding to a chain of  $(l-2)$  sites and a free boundary condition. The lowest wavefunction (boundstate) becomes localized at  $j = 1$  in this limit with eigenvalue  $-V$ .

The overlaps between the unperturbed,  $\psi$ , and perturbed,  $\tilde{\psi}$ , one-particle states assume the special form, reminiscent of the first-order perturbation theory, but actually exact (Appendix B):

$$\langle \tilde{\Psi}^m | \Psi^n \rangle = -V \frac{C(\tilde{k}_m)C(k_n)}{\epsilon(\tilde{k}_m) - \epsilon(k_n)}, \quad (3.15)$$

$$\langle \tilde{\Psi}^1 | \Psi^n \rangle = -V \frac{C_B C(k_n)}{\epsilon_B - \epsilon(k_n)}, \quad (3.16)$$

where

$$C(k) = \frac{\sqrt{2} \sin(l-1)k}{\sqrt{(l-1) - \sin(l-1)k \cos lk / \sin k}}, \quad (3.17)$$

$$C_B = \frac{\sqrt{2} \sinh(l-1)\kappa}{\sqrt{\sinh(l-1)\kappa \cosh l\kappa / \sinh \kappa - (l-1)}}. \quad (3.18)$$

#### IV. CALCULATION OF HOLE PROPAGATOR. COMPARISON TO THE CFT PREDICTIONS

The Green's function  $G(u)$  is determined by the set of matrix elements,

$$|\langle AB; m | \mathcal{O} | AA; 0 \rangle| \rightarrow \langle \tilde{\Phi}_{m;e,f} | \Phi_0 \rangle \equiv C_{e,f}^{0m} \quad (4.1)$$

between (perturbed and unperturbed) many-body states of the system and corresponding excitation energies,  $\Delta\epsilon_{m;e,f}$  (we note explicitly whether the boundstate if present is occupied ( $f$ ) or empty ( $e$ ), and label by  $m'$  the appropriate excited states of the band).

When there are  $N$  spinless noninteracting electrons in the system, the many-particle wave function is a  $N \times N$  Slater determinant

$$\Phi = \frac{1}{\sqrt{N!}} \det(\Psi_{l_a}^{(n_b)}). \quad (4.2)$$

Here  $\Psi_{l_a}^{(n_b)}$  is an appropriate one-particle eigenfunction of the state  $n_b$ , taken at the coordinate of the  $a$ th particle,  $a, b = 1, 2, \dots N$ .

The overlap of two such states is a determinant

$$(\tilde{\Phi}, \Phi) = \frac{1}{N!} \sum_{j_1} \dots \sum_{j_N} \det(\tilde{\Psi}_{j_n}^{(m)*}) \det(\Psi_{j_n}^{(m)}) \equiv \det((\tilde{\Psi}^{(m)}, \Psi^{(n)})). \quad (4.3)$$

The remarkable form of the one-particle overlaps (3.15,3.16) allows us to apply the Cauchy formula<sup>20</sup> in order to calculate the determinant (4.3):

$$\det\left(\frac{1}{a_m + b_n}\right) = \frac{\prod_{m>n}(a_m - a_n) \prod_{m>n}(b_m - b_n)}{\prod_{m,n}(a_m + b_n)} \quad (4.4)$$

Unlike the situation considered in the papers by Anderson and Combescot and Nozières<sup>10,6</sup>, in our model the special form of the overlaps is an exact result, and not the consequence of the linearization of the dispersion law close to Fermi surface.

We begin with calculating  $C_f^{00}$ , the overlap of the ground states of the system with and without the core potential, which yields the Anderson exponent (2.12). In the corresponding determinant

(4.3) both “old” and “new” indices run from  $n, m = 1$  to  $n, m = N$ . (That is, in the “new” state there is one bound electron and  $(N - 1)$  electrons in the band, and no  $e - h$  pairs). The other interesting overlap,  $C_f^{00}$ , corresponds to the situation when the bound state in the “new” system is empty, and all  $N$  electrons are in the band, occupying the lowest lying states (still no  $e - h$  pairs):  $n = 1, \dots, N$ , but  $m = 2, \dots, N + 1$ . It should yield the “empty boundstate” Anderson exponent, which according to general considerations<sup>4</sup> should be  $(1 - \frac{\delta_F}{\pi})^2$ , as distinct from the “filled” value  $(\frac{\delta_F}{\pi})^2$ . Using the Cauchy formula, we find

$$C_f^{00} = (-V)^N C_B \prod_{m=2}^N C(\tilde{\kappa}_m) \prod_{n=1}^N C(\kappa_n) \frac{\prod_{m>m'=1}^N (\tilde{\epsilon}_m - \tilde{\epsilon}_{m'}) \prod_{n>n'=1}^N (\epsilon_{n'} - \epsilon_n)}{\prod_{m=1}^N \prod_{n=1}^N (\tilde{\epsilon}_m - \epsilon_n)}; \quad (4.5)$$

$$C_e^{00} = (-V)^N \prod_{m=2}^{N+1} C(\tilde{\kappa}_m) \prod_{n=1}^N C(\kappa_n) \frac{\prod_{m>m'=2}^{N+1} (\tilde{\epsilon}_m - \tilde{\epsilon}_{m'}) \prod_{n>n'=1}^N (\epsilon_{n'} - \epsilon_n)}{\prod_{m=2}^{N+1} \prod_{n=1}^N (\tilde{\epsilon}_m - \epsilon_n)}, \quad (4.6)$$

and for their ratio:

$$R = \frac{C_e^{00}}{C_f^{00}} = \frac{C(\tilde{\kappa}_{N+1})}{C_B} \cdot \frac{\epsilon_1 - \tilde{\epsilon}_1}{\tilde{\epsilon}_{N+1} - \epsilon_1} \cdot \prod_{m=2}^N \frac{\tilde{\epsilon}_{N+1} - \tilde{\epsilon}_m}{\tilde{\epsilon}_{N+1} - \epsilon_m} \prod_{m=2}^N \frac{\epsilon_m - \tilde{\epsilon}_1}{\tilde{\epsilon}_m - \tilde{\epsilon}_1}. \quad (4.7)$$

Expression (4.7) is easily calculated for pretty large systems, since it involves the number of operations only of order  $l$ . The approximate values for the energies  $\tilde{E}_m$  can be accurately calculated as a perturbation series in  $t/V \ll 1$  (see Appendix B). If the above predictions are valid, then the ratio should depend on the system size as

$$R \propto (l-1)^{\frac{1}{2}} \left(\frac{\delta_F}{\pi}\right)^2 - \frac{1}{2} \left(1 - \frac{\delta_F}{\pi}\right)^2 = (l-1)^{\frac{\delta_F}{\pi} - \frac{1}{2}}. \quad (4.8)$$

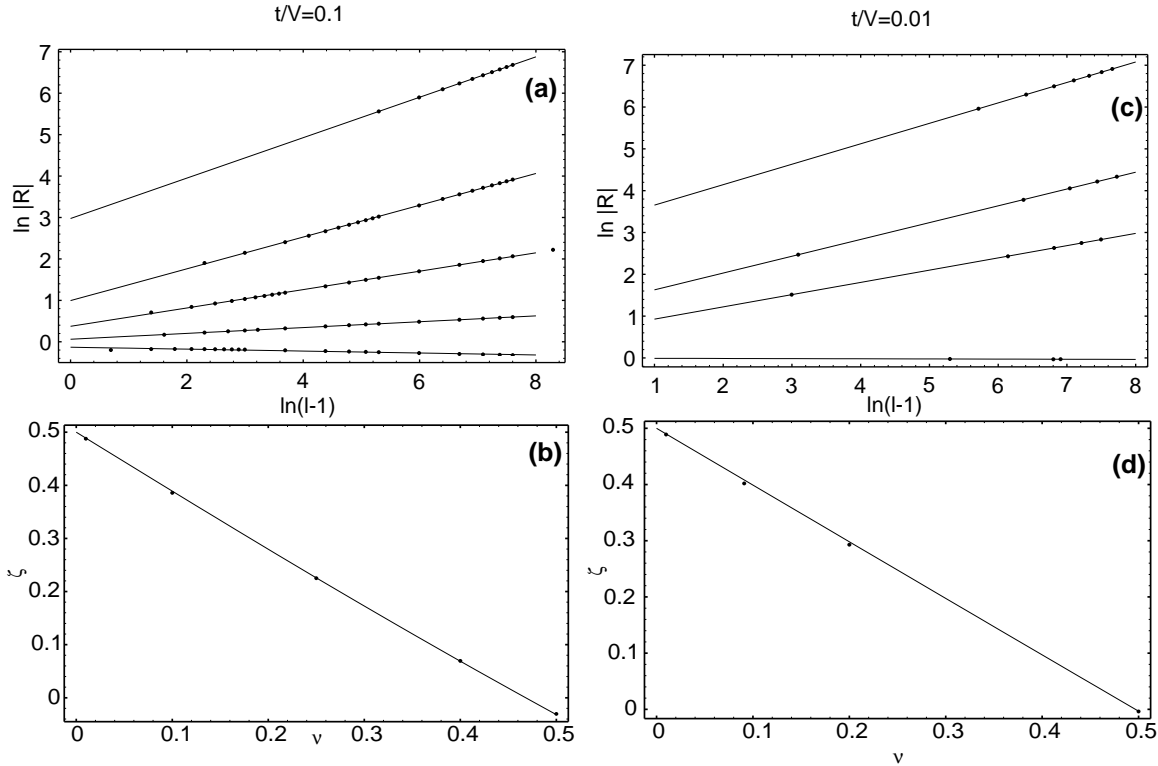


FIG. 2. (a) Logarithm of ratio  $|R| = |C_e^{00}/C_f^{00}|$  as a function of (even) chain length  $(l - 1)$  for  $t/V = 0.1$  and  $\nu = 1/2; 2/5; 1/4; 1/10$  and  $1/100$ ; the lines are best fits to points with  $(l - 1) > 10$  by  $\ln |R| = A + \zeta \ln(l - 1)$ ; (b) Exponent  $\zeta(\nu)$ . The curve is  $\frac{\delta(\nu; \frac{t}{V}=0.1)}{\pi} - \frac{1}{2}$ . (c) The same as (a) for  $t/V = 0.01$  and  $\nu = 1/2; 1/5; 1/11$  and  $1/101$  (in the latter three cases the length  $(l - 1)$  was chosen to be odd); the lines are best fits to points with  $(l - 1) > 10$  by  $\ln |R| = A + \zeta \ln(l - 1)$ ; (d) Exponent  $\zeta(\nu)$ . The curve is  $\frac{\delta(\nu; \frac{t}{V}=0.01)}{\pi} - \frac{1}{2}$ .



Here  $\delta_F$  is the phase shift at the Fermi surface,  $k_F = \pi\nu$ .

The results are shown in Fig.2 ( $t/V = 0.1$  and  $0.01$ ) for  $(l-1) \leq 4000$ . As is clear from the figures, the ratio as a function of  $l$  at fixed density  $\nu = \frac{N}{l-1}$  behaves as

$$R(l; \nu) \propto (l-1)^{\zeta(\nu)}, \quad (4.9)$$

where indeed (the least squares best fit parameters are shown in figure captions):

$$\zeta(\nu) \approx \frac{\delta_F(\nu; \frac{t}{V} = 0.01)}{\pi} - \frac{1}{2}, \quad (4.10)$$

for  $\frac{\delta_F(\nu)}{\pi} \approx \frac{1}{2} - \nu$ , as seen in Fig.1.

Calculation of the coefficients  $C_{f,e}^{00}$  themselves is more time consuming. We calculated  $C_e^{00}$  and  $C_f^{00}$  in the limit  $t/V \rightarrow 0$  for  $(l-1) \leq 400$ . The results are shown in Fig.3. The matrix elements dependence on size and density is accurately described by

$$C_{e,f}^{00}(l, \nu) = A_{e,f}(\nu)(l-1)^{-\frac{1}{2}} \left( \frac{\delta_F(\nu)}{\pi} \right)^2, \quad (4.11)$$

thus confirming the validity of the original Anderson's result<sup>10</sup> in the case of binding core potential and arbitrary electronic density.

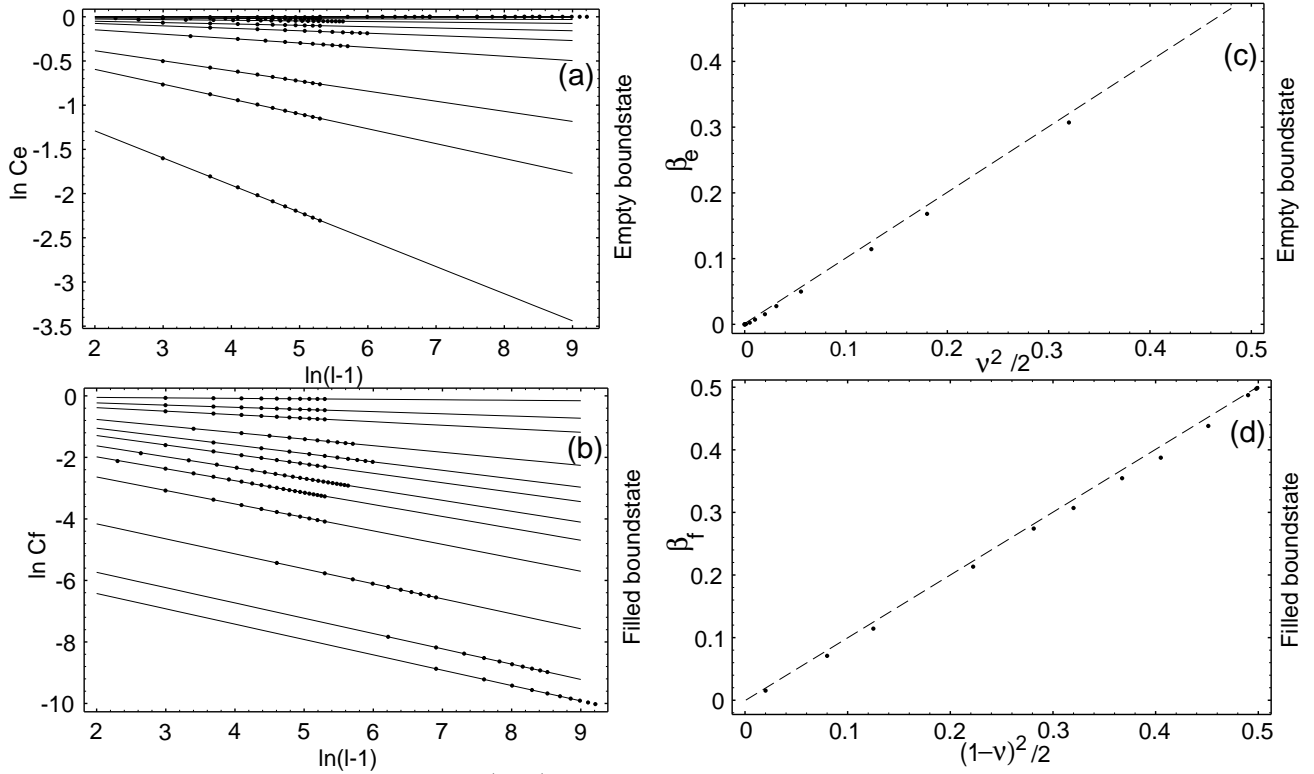


FIG. 3. (a) Logarithm of the coefficient  $|C_e^{00}|$  (empty boundstate) as a function of chain length for  $t/V \rightarrow 0$  and  $\nu = 1/1000; 1/500; 1/100; 1/20; 1/7; 1/5; 1/4; 1/3; 1/2; 3/5$  and  $4/5$ ; the lines are best fits to points with  $(l-1) > 10$  by  $C_e^{00}(l, \nu) = A_e(\nu)N^{-\beta_e(\nu)}$ ; (b) The same for  $|C_f^{00}|$  (filled boundstate). (c,d) Anderson exponents  $\beta_e$  (c) and  $\beta_f$  (d). The curves are  $\beta_e(\nu) = \frac{\nu^2}{2}$  and  $\beta_f(\nu) = \frac{(1-\nu)^2}{2}$ . (In the limit  $t/V = 0$ ,  $\nu = 1 - \delta/\pi$ .)

Turning to the contributions of the excited states,  $C_{f,e}^{0m'}$ , we must keep in mind that in the model, the degeneracy of energy levels in the CFT formula (2.15) is lifted. Therefore when checking Eq. (2.22), we calculate the ratios  $\frac{|\sum_m C_{e,f}^{0m}|^2}{|C_{e,f}^{00}|^2}$ , where the sum is extended over the excited states which would be degenerate in the case of linear dispersion relation. These clusters of nearly degenerate states are clearly seen in Fig. (4), where we plot  $\log f(E) = \log \sum_{\epsilon_m \leq E} |C_{e,f}^{0m}|^2$  vs.  $\log E$ . In fact,

not all excited states are included in Fig. (4), but only those corresponding to a single particle-hole excitation. In the large  $l$  limit, all excited states with energies  $\pi v_F m/l$  with  $m = 1, 2$  or  $3$ , discussed in Sec. II, correspond to single particle-hole excitations. However, multi particle-hole excitations begin to appear at  $m = 4$ . We might try to extract the FES exponent from the slope at low energies and large  $l$ , assuming that the neglected multi particle-hole excitations don't make too large a contribution close to the threshold. Assuming  $I \sim \omega^{-\alpha}$  in this region, then for small  $E$   $f(E) \sim E^{1-\alpha} \equiv E^\gamma$ . The tangent of the curve should yield the FES exponent-related  $\gamma = \left(\frac{\delta f}{f}\right)^2$ , but actually it is significantly smaller.

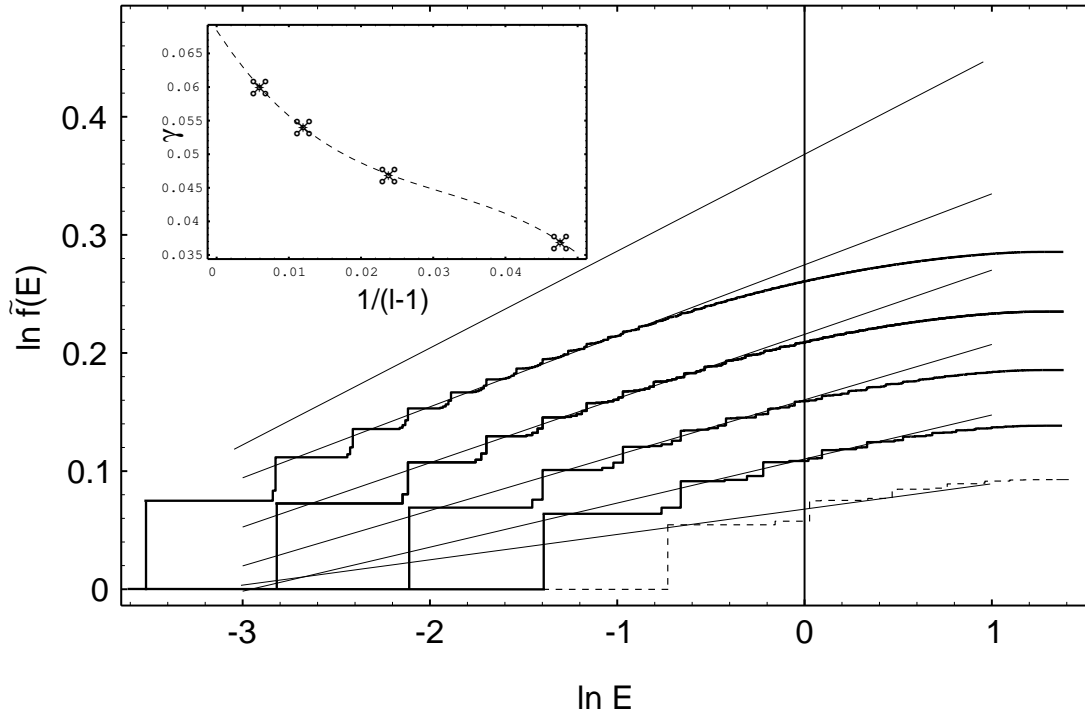


FIG. 4. The normalized integral of intensity,  $\tilde{f}(E) = \sum_{E_m \leq E} \frac{|C_e^{0m}|^2}{|C_e^{00}|^2} \propto \int_0^E I(\omega) d\omega$ , vs. energy, for the case of empty boundstate and  $t/V \rightarrow 0$ . Density  $\nu = 6/21$ ; system size  $(l-1) = 21; 42; 84; 168$ . The best fits yield  $\gamma = 0.037; 0.047; 0.054$  and  $0.060$  resp. The CFT value is  $0.082$  (uppermost line). The clusters of almost degenerate excited states are clearly seen (in one-pair approximation the  $n$ -th excited state is  $n$ -fold degenerate). The dotted line shows the direct diagonalization results by Eder and Sawatzky (Ref.( 14)), for  $t = 1, V = 32, N = 6, (l-1) = 21; \gamma = 0.021$ . Due to normalization to  $|C_e^{00}|^2$  the curves are offset in vertical direction; as the system size grows, the plateau heights are reaching the universal values predicted by CFT for the ratios of subsequent excited peak amplitudes to the lowest energy peak amplitude (see Eq.(2.22) and Fig.5). Inset: FES exponent vs. inverse chain length. The cubic extrapolation to infinite system size  $\gamma(0) = 0.068$  still falls short of the CFT value.

The calculations of the intensities of the first few peaks ( $t/V = 0.1$ ; Fig.5) shows that finite-size corrections to these amplitudes are significant for  $l \sim 400$ . Thus we shouldn't expect to be able to obtain the FES exponent reliably this way even if the neglect of multi particle-hole excitations was valid.

In Fig. (5) and the Table we show the ratio of the *total* amplitude of all peaks at excitation energy  $v_F \pi m/l$ , to the amplitude of the lowest peak ( $m = 0$ ) for  $m = 1, 2, 3$  for both filled and empty boundstate,  $R_m^{e,f}$ , following the discussion in Sec. II.  $t/V = .1$  and the maximum length considered was  $l = 400$ . The predictions for  $R_m^{e,f}$  from conformal field theory in Eq. (2.22) are also shown in the figures and table. The finite-size corrections to these ratios are quite large, but upon extrapolating in  $1/l$  we obtain good agreement with the CFT predictions in all six cases.

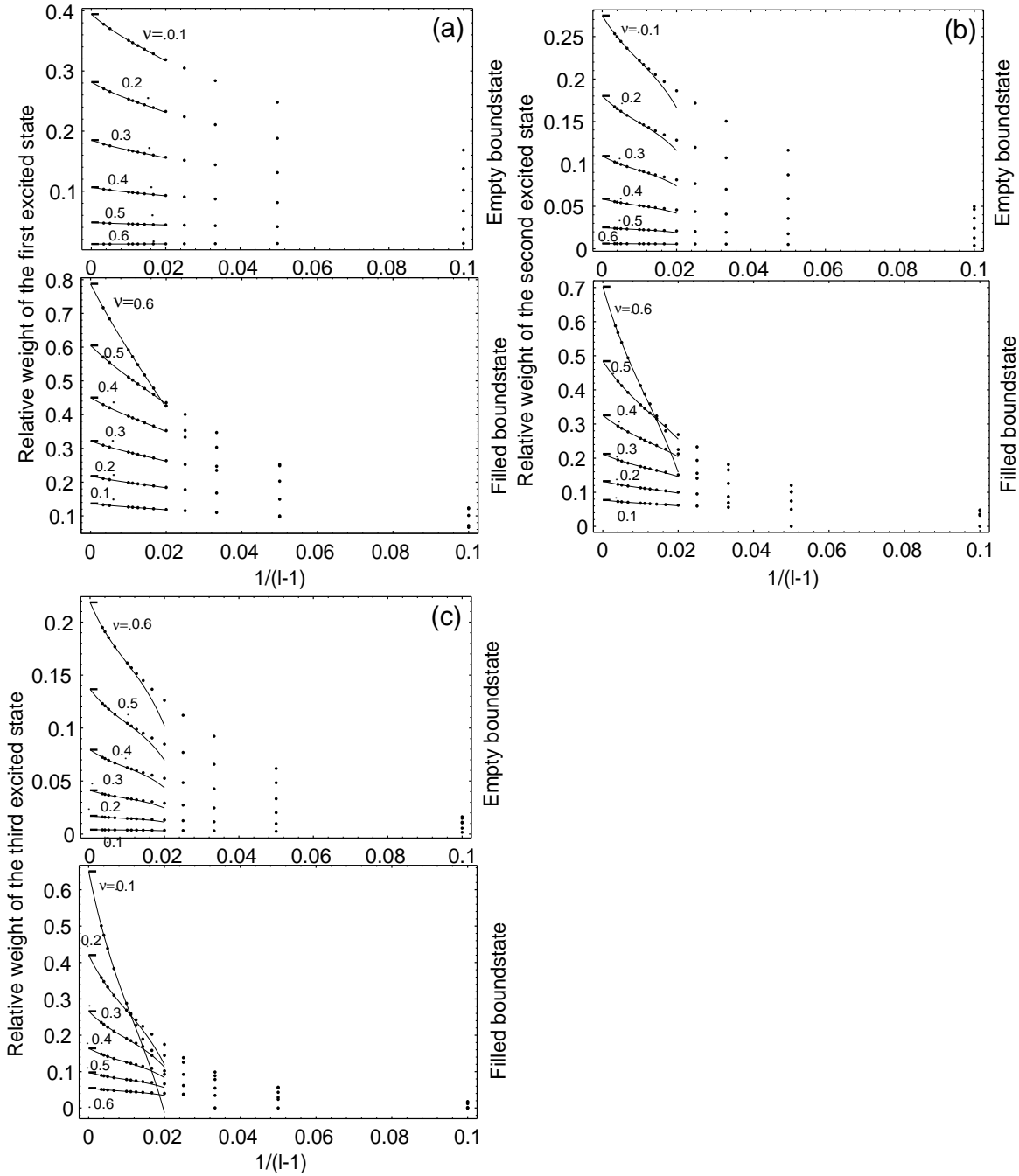


FIG. 5. (a) Relative weight of the first excited state peak in the hole propagator for different densities  $N/(l-1) = 0.1(0.1)0.6$ ;  $t/V = 0.1$ . The horizontal lines mark the CFT predictions (Eq.(2.22)), curves are the least squares' fits of the third-order in  $1/(l-1)$ , calculated from the four points with smallest  $1/(l-1)$ . Notice that these curves are in a good agreement with the data in a larger range of  $1/(l-1)$ . (b),(c) The same for the second and third excited states.

The finite size corrections, at a fixed value of  $l$ , are roughly proportional to  $\left(\frac{\tilde{\delta}_F}{\pi}\right)^2$ , where the effective phase shift in the presence of bound state is  $\tilde{\delta}_F = \delta_F$  if the boundstate is filled, and  $\pi - \delta_F$ , if it is empty<sup>6,4</sup>. Thus CFT predictions in a finite system with filled boundstate are more accurate for low density than for high density, and the opposite for empty boundstate.

## V. SUM RULES AND OPEN QUESTIONS

The Fourier transform of the core hole Green's function, proportional to the photoemission intensity, can be written:

$$I(\omega, \nu) = \sum_n |\langle 0 | \tilde{n} \rangle|^2 \delta(\tilde{E}_n - E_0 - \omega), \quad (5.1)$$

where  $|\tilde{n}\rangle$ ,  $\tilde{E}_n$  label all states of the system with the core hole potential turned on and  $|0\rangle$ ,  $E_0$  refers to the groundstate without the core hole potential. Here we make explicit the fact that  $I$  depends on the electron density (i.e.  $k_F$ ). The states  $|\tilde{n}\rangle$  can be classified according to whether the boundstate is filled or empty and accordingly we may decompose  $I(\omega)$ :

$$I(\omega, \nu) = I_f(\omega, \nu) + I_e(\omega, \nu). \quad (5.2)$$

Near a threshold,  $I(\omega, \nu)$  takes the form:

$$I(\omega, \nu) = F(\nu)(\omega - \omega_0)^{-\alpha(\nu)}. \quad (5.3)$$

So far, we have focussed on the value of the FES exponent,  $\alpha(\nu)$ . In this section we would also like to consider the dependence of the amplitude factor,  $F$  on the density and also the behaviour of  $I(\omega, \nu)$  away from the threshold. While most of this behaviour is clearly non-universal, one might expect certain universal features to immerge in the limit  $\nu \rightarrow 0$ . Our interest in this limit is motivated by the experiments on doped semiconductors.<sup>18</sup>

To begin with we point out the existence of two sum rules. These apply very generally to FES problems in arbitrary dimensions, without any particular assumptions about spherical symmetry or about the location of the core potential in the one-dimensional case. It follows from completeness of the states  $|\tilde{n}\rangle$  that  $I(\omega)$  obeys the sum rule:

$$\int_{-\infty}^{\infty} d\omega I(\omega, \nu) = 1. \quad (5.4)$$

This implies that the integrated intensities from the states with filled or empty boundstate obey:

$$I_f + I_e = 1. \quad (5.5)$$

Another useful sum rule can be derived by writing  $I_f(\omega, \nu)$  in terms of the projection operator,  $\hat{n}_B$  onto states in which the boundstate is occupied:

$$\int d\omega I_f(\omega, \nu) = \sum_n |\langle 0 | \hat{n}_B | \tilde{n} \rangle|^2 = \langle 0 | \hat{n}_B | 0 \rangle. \quad (5.6)$$

We may write

$$\hat{n}_B = \psi_B^\dagger \psi_B, \quad (5.7)$$

where  $\psi_B$  annihilates the boundstate electron.  $\psi_B$  can be expressed in terms of the operator  $\psi_j$  which annihilates an electron at site  $j$  and the boundstate wave-function,  $\Psi_j^B$ :

$$\psi_B = \sum_j \Psi_j^B \psi_j. \quad (5.8)$$

Thus:

$$I_f = \sum_{i,j} \Psi_i^B \Psi_j^B \langle 0 | \psi_i^\dagger \psi_j | 0 \rangle. \quad (5.9)$$

In a d-dimensional continuum formulation this becomes:

$$I_f = \int d^d \vec{r} d^d \vec{r}' \Psi^B(\vec{r}) \Psi^B(\vec{r}') \langle 0 | \psi^\dagger(\vec{r}) \psi(\vec{r}') | 0 \rangle. \quad (5.10)$$

At this point, it is convenient to Fourier expand the position-space annihilation operators. The form of this expansion depends somewhat on the boundary conditions (in the system without the core potential). In dimension  $d > 1$  we generally consider a translationally system in which case:

$$\psi_{\vec{r}} = \int \frac{d^d \vec{k}}{(2\pi)^d} e^{i\vec{k}\cdot\vec{r}} \psi_{\vec{k}}. \quad (5.11)$$

In this case, the sum rule becomes:

$$I_f = \int \frac{d^d k}{(2\pi)^d} |\Psi^B(\vec{k})|^2 \theta(\epsilon_F - \epsilon_{\vec{k}}), \quad (5.12)$$

where  $\Psi^B(\vec{k})$  is the Fourier transform of the boundstate wavefunction. The  $\vec{k}$ -integral is only over states below the Fermi surface. This makes it clear that  $I_f$  vanishes as  $\nu \rightarrow 0$ , and approaches 1 as  $\nu \rightarrow 1$ . Roughly speaking, when the density is small, there is a negligible probability of an electron being near the origin when the core potential is switched on so the overlap of the unperturbed groundstate with any state in which the boundstate is occupied goes to 0. In the opposite limit of high density there is probability near 1 of an electron being near the origin. It is interesting to consider how rapidly  $I_f$  vanishes as  $\nu \rightarrow 0$ . If we assume that the dispersion relation and core potential are spherically symmetry, then we may classify the boundstate by its principle angular momentum quantum number,  $L$ . At small  $k$ ,  $\Psi^B(\vec{k}) \propto k^L$ , so

$$I_f \propto k_F^{2L+d} \propto \nu^{1+2L/d}. \quad (5.13)$$

In a one-dimensional translationally invariant system with reflection symmetry the boundstate can be classified as being an even or odd function of  $x$ .  $I_f \propto \nu$  for an even boundstate or  $\nu^3$  for an odd boundstate. When the potential is at the end of a one-dimensional chain with a free boundary condition,

$$\Psi^B(k) \equiv \sum_{j=1}^{l-1} \sin kj \psi_j^B. \quad (5.14)$$

Thus  $\Psi^B(k) \propto k$  as  $k \rightarrow 0$ , so  $I_f \propto \nu^3$ .

The behaviour of the FES exponent,  $\alpha$  at  $\nu \rightarrow 0$  follows, in some cases, from Levinson's theorem, which determines the behaviour of the phase shift as  $k \rightarrow 0$ . For an s-wave boundstate, or for a one-dimensional problem with the impurity at the end of the chain, the phase shift approaches  $\pi$  at the bottom of the band when there is a boundstate. Thus it follows, from Eqs. (2.17), (2.20) and (2.21) that  $\alpha_f \rightarrow 0$  and  $\alpha_e \rightarrow 1$ . Thus  $I_f(\omega)$  becomes a step function near its threshold and  $I_e(\omega)$  becomes a  $\delta$ -function. [ $\alpha = 1$  corresponds to a constant Green's function in the time-domain whose Fourier transform gives a  $\delta$ -function.] Thus  $I_e(\omega, \nu)$  approaches, in the  $\nu \rightarrow 0$  limit, the result for the empty system: a  $\delta$ -function of unit intensity. This follows since the groundstate with no electrons is the same with or without the core potential; it is simply the vacuum state. Thus we expect

$$F_e(\nu) \rightarrow 1, \quad (\nu \rightarrow 0). \quad (5.15)$$

The step in  $I_f(\omega, \nu)$  corresponds to electrons from the continuum falling into the boundstate after it is created. The probability for this process, and hence  $F_f(\nu)$  should vanish as  $\nu \rightarrow 0$ .

We have been unable to understand, from general arguments, how  $F_f(\nu)$  approaches 0 or how  $F_e(\nu)$  approaches 1 as  $\nu \rightarrow 0$ . More generally, we would like to know how the functions  $I_e(\omega)$  and  $I_f(\omega)$  behave even away from the threshold as  $\nu \rightarrow 0$ . In particular, it is interesting to ask whether there might be some sort of universal scaling form in that limit. This behaviour is only weakly constrained by the above sum rules.

It is interesting to investigate these questions numerically. For a finite system,  $I(\omega, \nu)$  is a sum of  $\delta$ -functions corresponding to the discrete finite size spectrum. For a large system the intensities of the first few peaks, with the boundstate filled or empty, will all be proportional to  $F_f(\nu)$  or  $F_e(\nu)$  respectively. This follows immediately from the conformal transformation of Sec. II. Thus we may conveniently determined  $F_{f,e}(\nu)$  numerically, for a large finite system, from the groundstate overlap (Anderson orthogonality calculation). That is:

$$|\langle 0|\tilde{0}\rangle|^2 = F(\nu) \left(\frac{\pi}{l}\right)^{2x}. \quad (5.16)$$

The resulting functions,  $F_{f,e}(\nu)$  are plotted in Fig. (6) for the special tight-binding model considered in the previous two sections, in the limit  $t/V \rightarrow 0$ . These are obtained from the intercepts of the curves in Fig.3. As can be seen from Fig.7, at small  $\nu$ ,

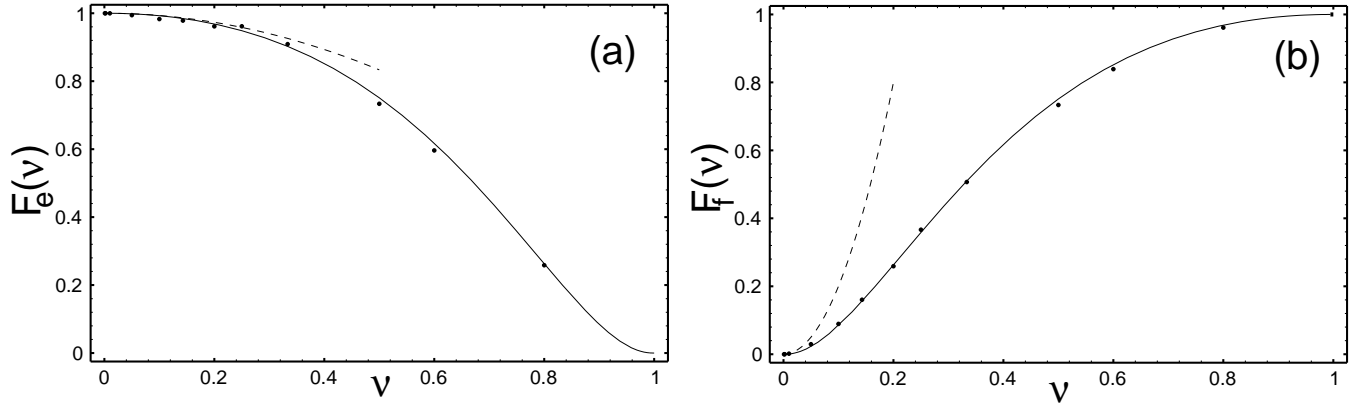


FIG. 6. FES amplitude as a function of density. The values of  $F_e$  (a) and  $F_f$  (b) are plotted vs.  $\nu$ . The curves are  $F_e^*(\nu) = (1 - \nu)^{2(1-(1-\nu)^{1/3})}$  and  $F_f^*(\nu) = \nu^{2(1-\nu^{1/3})}$ . Dotted lines represent  $1 - 2\nu^2/3$  and  $20\nu^2$  resp. (see text)

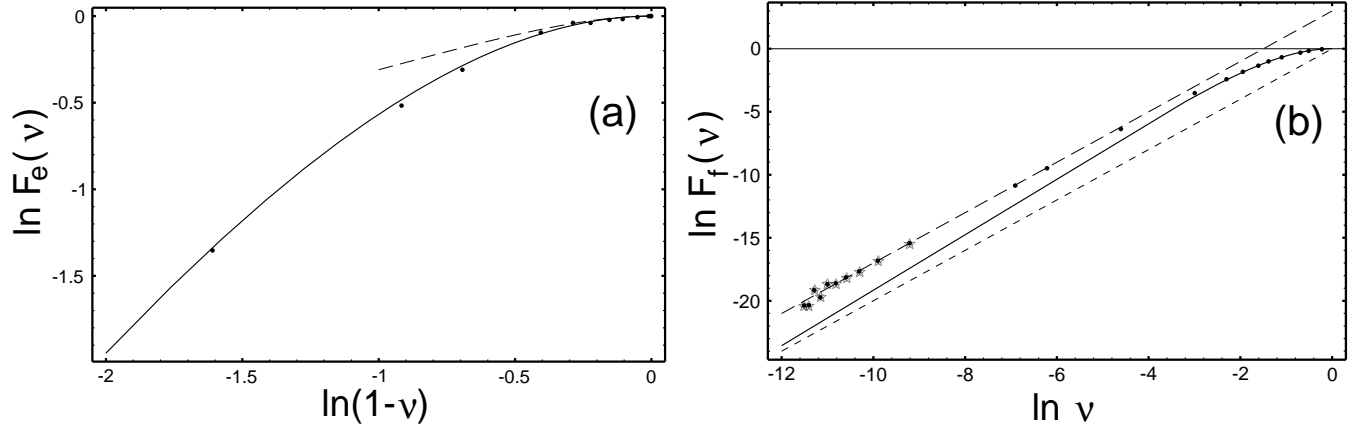


FIG. 7. FES amplitudes at low densities. In (b) stars represent the data not shown in Fig.6(b); the relation  $F_f(\nu) \approx 20\nu^2$ , the upper dashed line, is clearly seen. The lower dotted line is  $\nu^2$ , the asymptotics of  $F_f^*(\nu)$  at  $\nu \rightarrow 0$ .

$$\begin{aligned} F_f(\nu) &\rightarrow 20\nu^2 \\ F_e(\nu) &\rightarrow 1 - (2/3)\nu^2. \end{aligned} \quad (5.17)$$

The former equation suggests the scaling hypothesis:

$$I_f(\omega, \nu) \rightarrow \nu^2 f[(\omega - \omega_0)/\nu], \quad (5.18)$$

for some scaling function  $f$ . This is consistent with the sum rule since:

$$\int_{\omega_0}^{\infty} d\omega I(\omega) = \nu^3 \int_0^{\infty} dx f(x) \propto \nu^3. \quad (5.19)$$

In the  $\nu \rightarrow 0$  limit, the threshold frequency  $\omega_0$  approaches  $\epsilon_B - \epsilon_0$ , the binding energy measured from the bottom of the band. The function  $f(x)$  must approach a constant at the threshold,  $x \rightarrow 0$ , consistent with the behaviour of the FES exponent  $\alpha_f \rightarrow 0$  as  $\nu \rightarrow 0$ . At large frequencies the function  $f$  must vanish sufficiently rapidly for the integral to converge. Apparently the scale over which  $I(\omega)$  varies is set by  $\nu \propto v_F$ . If this is also the relevant energy scale for a translationally invariant one-dimensional system, or a higher dimensional  $s$ -wave boundstate, then we would expect the behaviour:

$$I(\omega, v_F) \propto f[(\omega - \omega_0)/v_F], \quad (5.20)$$

consistent with the sum rule. That is, the threshold peak has a fixed amplitude, but the energy scale over which  $I(\omega)$  decreases scales to 0 as  $\nu \rightarrow 0$ . [We can speculate that in our model, due to the suppression of the wave function near the end of the chain, the extra factor of  $\nu^2$  appears in the expression for  $I_f$ , which would be absent in the  $s$ -wave channel of a higher-dimension system, where

the sum rule should yield  $\nu$  instead of  $\nu^3$ .] It would be interesting to investigate this behaviour in more general models.

For almost all values of  $\nu$  we found that  $F_{f,e}$  are well described, for our special model, by the functions

$$F_f^*(\nu) = \nu^{2(1-3\sqrt{\nu})}; \quad F_e^*(\nu) = (1-\nu)^{2(1-3\sqrt{1-\nu})}, \quad (5.21)$$

as shown in Figs.6,7. (In two dimensions the dependence  $F_f(\nu) \sim \nu^{2(1-\nu^a)}$  could be expected from calculations based on the linked cluster approximation<sup>22</sup>, but with  $a = 2$ , not  $1/3$ .) At very low densities  $F_e(\nu)$  is still well described by (5.21), as evident from (5.17) and Fig.6, while  $F_f(\nu)$  approaches the  $20\nu^2$ -dependence of (5.17) (see Fig.7).

## VI. CONCLUSIONS

We have investigated the Anderson orthogonality catastrophe and Fermi edge singularity in photoemission spectrum in a tractable 1D tight-binding model of spinless electrons, in the case where the core potential produces a boundstate.

We have confirmed the predicted relation between the scattering phase on the Fermi surface,  $\tilde{\delta}_F$ , and the Anderson and FES exponents. We have calculated the ratios of intensities of discrete adsorption peaks for a finite system, using CFT and checked the formulas at both primary and secondary thresholds numerically. We have found that the higher order finite size corrections are roughly proportional to  $\tilde{\delta}_F^2$  and can be significant in a system as large as several hundred sites. Thus they might be observable in a mesoscopic system. The CFT-based relation between the exponents and  $O(1/l)$ -term in the ground state energy shift was confirmed as well. Using the model, we obtained the explicit density dependence of the FES amplitude in the whole range of  $\nu$ .

## ACKNOWLEDGMENTS

We would like to thank G. Sawatzky, J. Young, and R. Eder for stimulating discussions and for acquainting us with their results prior to publication. A.Z. is grateful to P. Hawrylak for interesting discussions and hospitality during his visit to IMS-NRC. This research was supported by NSERC.

Empty boundstate	$\nu$	0.1	0.2	0.3	0.4	0.5	0.6
$m = 1$	$(\delta_F/\pi - 1)^2$	0.0123	0.0485	0.1071	0.1859	0.2827	0.3960
	relative weight	0.0122	0.0483	0.1067	0.1851	0.2816	0.3944
$m = 2$	$\frac{1}{2}(\delta_F/\pi - 1)^2 \cdot (1 + (\delta_F/\pi - 1)^2)$	0.0062	0.0254	0.0593	0.1102	0.1813	0.2764
	relative weight	0.0062	0.0253	0.0589	0.1095	0.1802	0.2747
$m = 3$	$\frac{1}{6}(\delta_F/\pi - 1)^2(1 + (\delta_F/\pi - 1)^2) \cdot (2 + (\delta_F/\pi - 1)^2)$	0.0042	0.0174	0.0417	0.0803	0.1380	0.2207
	relative weight	0.0041	0.0172	0.0412	0.0795	0.1367	0.2187
Filled boundstate	$\nu$	0.1	0.2	0.3	0.4	0.5	0.6
$m = 1$	$(\delta_F/\pi)^2$	0.7906	0.6079	0.4525	0.3236	0.2193	0.1374
	relative weight	0.7868	0.6051	0.4505	0.3222	0.2184	0.1369
$m = 2$	$\frac{1}{2}(\delta_F/\pi)^2 \cdot (1 + (\delta_F/\pi)^2)$	0.7078	0.4887	0.3287	0.2142	0.1337	0.0782
	relative weight	0.7025	0.4853	0.3264	0.2128	0.1329	0.0777
$m = 3$	$\frac{1}{6}(\delta_F/\pi)^2(1 + (\delta_F/\pi)^2) \cdot (2 + (\delta_F/\pi)^2)$	0.6584	0.4248	0.2687	0.1659	0.0989	0.0557
	relative weight	0.6505	0.4202	0.2659	0.1642	0.0980	0.0552

TABLE I. Relative weights of first  $m$  excited peaks in the hole propagator compared to CFT predictions of Eq.(2.22). The relative weights in the limit  $l \rightarrow \infty$  are obtained from the best fit to the finite-size values (Fig.7),  $w(l) = c_0 + c_1/(l-1) + c_2/(l-1)^2 + c_3/(l-1)^3$  using the method of the least squares to determine  $c_{0,\dots,4}$  from the *four* points with smallest  $1/(l-1)$  for each graph.  $w(\infty) = c_0$ .



## APPENDIX A: FINITE SIZE ENERGY

In this appendix we wish to demonstrate explicitly the formula relating the finite size correction to the groundstate energy difference to the phase shift at the Fermi surface. At the same time we will expose a subtlety in the definition of the  $O(1/l)$  term in this energy difference. This groundstate energy difference contains a dominant term of  $O(1)$ . This is non-universal, depending on the ultraviolet cut-off in the Dirac fermion theory. It must be subtracted correctly to determine the universal  $O(1/l)$  correction. To be concrete, we consider a tight-binding chain of  $l-1$  sites,  $j = 1, 2, 3, \dots, l-1$  with free boundary conditions,  $N$  electrons and a scattering potential,  $V_j$ , localized near  $j = 0$ .

$$H = - \sum_{j=1}^{l-2} (t\psi_j^\dagger \psi_{j+1} + \text{h.c.} + V_j \psi_j^\dagger \psi_j) \quad (\text{A1})$$

When  $V_j = 0$  the single particle eigenstates are  $\sin kj$ . A simple way of determining the allowed wave-vectors,  $k$ , is to imagine adding two ‘‘phantom sites’’ at  $j = 0$  and  $j = l$  and then imposing the boundary condition:

$$\psi_0 = \psi_l = 0. \quad (\text{A2})$$

The Fourier expansion of  $\psi_j$  in terms of creation and annihilation operators then involves  $\sin(kj)$  with:

$$k_n = \pi n/l, \quad m = 1, 2, 3, \dots, l-1. \quad (\text{A3})$$

The groundstate energy for  $V = 0$  is:

$$E_0 = \sum_{m=1}^{l-1} \epsilon(k_m), \quad (\text{A4})$$

with  $\epsilon(k) = -2t \cos k$ . In fact, this discussion doesn’t depend on the form of  $\epsilon(k)$  and can be applied immediately to a more general Hamiltonian with longer range hopping provided that the boundary condition of Eq. (A2) applies. The only property of  $\epsilon(k)$  that we will use is that its derivative vanishes at  $k = 0$ .

In the  $l \rightarrow \infty$  limit, the Fermi wave-vector is

$$k_F = \pi \lim_{l \rightarrow \infty} N/l. \quad (\text{A5})$$

For a finite system, there is an ambiguity of  $O(1/l)$  in the definition of  $k_F$  since it may be chosen anywhere between  $\pi N/l$  and  $\pi(N+1)/l$ . It turns out to be convenient to choose it to lie exactly halfway between the  $N^{\text{th}}$  and  $l^{\text{st}}$  level:

$$k_F \equiv \pi(N+1/2)/l. \quad (\text{A6})$$

This gives the model an approximate particle-hole symmetry, in the vicinity of the Fermi surface. [Only at half-filling does this particle-hole symmetry become exact.] We regard  $k_F$  as being held fixed as  $l$  is varied, for purposes of determining the term of  $O(1/l)$  in the groundstate energy. Thus the quantity  $(N+1/2)/l$  must be held fixed. In practice, for numerical simulations, this is not particularly more nor less difficult than holding fixed the actual density,  $N/(l-1)$ . For instance, to obtain  $k_F = \pi/4$  we may choose the number of sites  $l-1 = 4N+1$  for arbitrary positive integer  $N$ .

The continuum limit Dirac theory is defined by only keeping wave-vectors near  $\pm k_F$ , writing:

$$\psi_j \approx e^{-ik_F j} \psi_L(j) + e^{ik_F j} \psi_R(j), \quad (\text{A7})$$

where  $\psi_{L,R}$  are left and right moving Dirac fields. The boundary conditions of Eq. (A2) imply:

$$\begin{aligned} \psi_L(0) + \psi_R(0) &= 0 \\ e^{-ik_F l} \psi_L(l) + e^{ik_F l} \psi_R(l) &= 0. \end{aligned} \quad (\text{A8})$$

Using Eq. (A6) the last equation gives:

$$\psi_L(l) - \psi_R(l) = 0, \quad (\text{A9})$$

corresponding to the “same” boundary conditions at both ends as discussed in Section II.  $k_F$  was chosen in Eq. (A6) above in order to obtain this boundary condition on the Dirac fermion.

Including the scattering potential,  $V_j$ , the single-particle eigenstates still become asymptotically plane waves,  $\sin[\tilde{k}j + \delta(\tilde{k})]$  (at distances large compared to the range of  $V$ ), where  $\delta(\tilde{k})$  is the phase shift. Thus the allowed wave-vectors are now:

$$\tilde{k}_n = k_n - \delta(\tilde{k}_n)/l, \quad (\text{A10})$$

with  $k_n \equiv \pi n/l$ . It is important to note that the argument of  $\delta$  in Eq. (A10) is  $\tilde{k}_n$ , not  $k_n$ . Thus, to  $O(1/l^2)$ , we may write:

$$\tilde{k}_n \equiv f(k_n) = k_n - \delta(k_n)/l + \delta'(k_n)\delta(k_n)/l^2. \quad (\text{A11})$$

The groundstate energy can thus be written:

$$E_0 = \sum_{n=1}^{l-1} \epsilon[\tilde{k}_n]. \quad (\text{A12})$$

This can be evaluated using the Euler-MacLaurin expansion:

$$\sum_{m=1}^{l-1} F(m - 1/2) = \int_0^{l-1} dx F(x) - \frac{1}{24} [F'(N) - F'(0)] + O(F''). \quad (\text{A13})$$

Setting:

$$F(n - 1/2) = \epsilon[f(\pi n/l)], \quad (\text{A14})$$

where the function,  $f$  is given by Eq. (A11), we obtain the convenient result,

$$F(N) = \epsilon[f(k_F)]. \quad (\text{A15})$$

Thus, to  $O(1/l)$ :

$$E_0 = \int_0^{l-1} dn \epsilon\{f[\pi(n + 1/2)/l]\} - v_F \pi / (24l), \quad (\text{A16})$$

where

$$v_F \equiv \epsilon'(k_F), \quad (\text{A17})$$

and corrections of  $O(1/l^2)$  have been dropped. Now it is convenient to change integration variables to:

$$k = \pi(n + 1/2)/l, \quad (\text{A18})$$

giving:

$$E_0 = l \int_0^{k_F} \frac{dk}{\pi} \epsilon[f(k)] - \frac{v_F \pi}{24l}. \quad (\text{A19})$$

Here the lower limit of integration has been shifted by  $\pi/2l$ . This is justified since  $\epsilon(k)$  is quadratic at  $k \rightarrow 0$ , producing only corrections of  $O(1/l^2)$  to  $E_0$ . Using Eq. (A11) and expanding to  $O(1/l)$  we obtain:

$$E_0 = l \int_0^{k_F} \frac{dk}{\pi} \left[ \epsilon(k) - \frac{\epsilon'(k)\delta(k)}{l} + \frac{\epsilon''(k)\delta^2(k)}{2l^2} + \frac{\epsilon'(k)\delta'(k)\delta(k)}{l^2} \right] - \frac{v_F \pi}{24l} \quad (\text{A20})$$

Integrating by parts, and using  $\epsilon'(0) = 0$ , we finally obtain:

$$E_0 = l \int_0^{k_F} \frac{dk}{\pi} \epsilon(k) - \frac{1}{\pi} \int_{\epsilon_0}^{\epsilon_F} d\epsilon \delta(\epsilon) + \frac{\pi v_F}{l} \left\{ \frac{1}{2} \left[ \frac{\delta(k_F)}{\pi} \right]^2 - \frac{1}{24} \right\} + O\left(\frac{1}{l^2}\right). \quad (\text{A21})$$

Here  $\epsilon_0 \equiv \epsilon(0)$  and  $\epsilon_F \equiv \epsilon(k_F)$ . The first term, of  $O(l)$  is the bulk groundstate energy. The second term of  $O(1)$  is a well-known result referred to as Fumi's theorem. Note that these terms depend on  $\epsilon$  and  $\delta$  over the whole band. On the other hand, the final term, of  $O(1/l)$  depends

only on data right at the Fermi surface, namely  $v_F$  and  $\delta(k_F)$ . The  $1/24$  term is the well-known conformal field theory result for open boundary conditions. The additional  $[\delta(k_F)/\pi]^2$  term gives the effect on the groundstate energy of changing the boundary conditions. This formula can be checked for the nearest neighbour model, with  $\epsilon(k) = 2t \cos(k)$ , and free boundary conditions. The exact groundstate energy is given by a geometric series:

$$\begin{aligned} E_0 &= t - \frac{t \sin k_F}{\sin(\pi/2l)} \\ &= \frac{l}{\pi} v_F + t - \frac{\pi v_F}{24l} + O(1/l^2), \end{aligned} \tag{A22}$$

with  $v_F \equiv 2t \sin k_F$ .

We note that adopting a different definition of  $k_F$ , such as  $\pi N/(l-1)$  in the one dimensional model, corresponds to adding a  $k$ -independent term to the phase shift  $[(\nu-1/2)]$ , where  $\nu$  is the density, in this case]. Eq. (A22) still holds, when written in terms of this redefined phase shift. This discussion was given for the case of a one dimensional tight-binding model with free ends but it can be easily generalized, for example to the s-wave sector of a three dimensional spherically symmetric continuum model with a vanishing boundary condition on the surface of a sphere if radius,  $l$ . With an appropriate definition of  $k_F$  [essentially defining, to  $O(1/l)$  what is held fixed as  $l$  is varied], Eq. (A22) is again obtained.

We can easily generalize Eq. (A22) to calculate the energy of a state with  $n$  extra electrons added, with  $n$  held fixed as  $N$  and  $l \rightarrow \infty$ . This gives:

$$\begin{aligned} E_n &= E_0 + \sum_{m=1}^n \epsilon[k_F - \delta(k_F)/l + \pi(m-1/2)/l] \\ &= E_0 + n\epsilon_F + (v_F \pi/l) \sum_{m=1}^n (m-1/2 - \delta(k_F)/\pi) + O(1/l^2). \end{aligned} \tag{A23}$$

Hence

$$E_n = l \int_0^{k_F} \frac{dk}{\pi} \epsilon(k) - \frac{1}{\pi} \int_{\epsilon_0}^{\epsilon_F} d\epsilon \delta(\epsilon) + n\epsilon_F + \frac{\pi v_F}{l} \left\{ \frac{1}{2} \left[ n - \frac{\delta(k_F)}{\pi} \right]^2 - \frac{1}{24} \right\} + O\left(\frac{1}{l^2}\right). \tag{A24}$$

## APPENDIX B: DISPERSION LAW AND WAVE FUNCTIONS IN A 1D TIGHT-BINDING CHAIN

Here we calculate exactly the phase shift, finite size spectrum, eigenstates and overlaps for the one-dimensional tight-binding model with an impurity potential at one end, given in Eq. (3.1).

It can be easily seen that the eigenstates can be written exactly in the form:

$$\Psi_j \propto \sin k(j-l). \tag{B1}$$

This wavefunction trivially satisfies the lattice Schroedinger equation (for arbitrary  $k$ ) at all sites  $2, 3, \dots, l-1$ , with:

$$\epsilon(k) = -2t \cos k. \tag{B2}$$

The Schroedinger equation for the first site determines the allowed values of  $k$ :

$$-t\Psi_2 - V\Psi_1 = \epsilon\Psi_1. \tag{B3}$$

Inserting Eq. (B1) and (B2), we obtain:

$$\frac{\sin k(l-1)}{\sin kl} = \frac{t}{V}. \tag{B4}$$

For sufficiently large  $V/t$  there is also a boundstate with wavefunction:

$$\chi_j \propto \sinh \kappa(l-j), \tag{B5}$$

where  $\kappa > 0$  in order that the wavefunction decreases with increasing  $j$ . This has energy:

$$\epsilon_B = -2t \cosh \kappa. \quad (\text{B6})$$

Again the Schroedinger equation is satisfied automatically (for any  $\kappa$ ) at all sites except the first which gives the condition determining  $\kappa$ :

$$\frac{\sinh \kappa(l-1)}{\sinh \kappa l} = \frac{t}{V}. \quad (\text{B7})$$

For  $l \gg 1$ , this gives:

$$e^{-\kappa} = t/V. \quad (\text{B8})$$

Since  $\kappa$  must be positive, we see that there is only a boundstate solution for  $V > t$ . In this case:

$$\epsilon_B = -(V + t^2/V). \quad (\text{B9})$$

For the continuum states we may calculate the exact phase shift, defined by the form of the wavefunction for  $l \gg 1$ :

$$\Psi_j \propto \sin[kj + \delta(k)]. \quad (\text{B10})$$

From Eq. (B1) we see that:

$$-kl = \delta(k) + \pi n, \quad (\text{B11})$$

for some integer  $n$ , in the limit  $l \rightarrow \infty$ . Substituting this into Eq. (B4), we obtain:

$$\frac{\sin[\delta(k) + k]}{\sin[\delta(k)]} = \frac{t}{V}. \quad (\text{B12})$$

This gives:

$$\delta = \arctan \left[ \frac{\sin k}{t/V - \cos k} \right]. \quad (\text{B13})$$

We now consider in more detail the spectrum of the finite system, of  $l-1$  sites. With no potential, there are  $l-1$  band wave-functions with:

$$k_n = n\pi/l, \quad n = 1, 2, 3, \dots (l-1). \quad (\text{B14})$$

Including the attractive potential, we see from Eq. (B7) that there is a solution of the form  $\sinh \kappa(j-l)$  for  $t/V < 1 - 1/l$ . We label this solution  $\tilde{\epsilon}_1$  and  $\tilde{\Psi}^1$ . For this range of  $t/V$  Eq. (B4) has only  $l-2$  solutions,  $\tilde{k}_2, \tilde{k}_3, \dots \tilde{k}_{l-1}$ . In particular, for  $V/t \rightarrow \infty$ , these  $l-2$  solutions become:  $\tilde{k}_n = (n-1)\pi/(l-1)$ , corresponding to a chain with free boundary condition at both ends and  $l-2$  sites.

The normalization of the band states can be calculated exactly in terms of  $\tilde{k}$  using:

$$\sum_{j=1}^{l-1} \sin^2 k(j-l) = \frac{1}{2} \left[ (l-1) - \frac{\sin k(l-1) \cos kl}{\sin k} \right]. \quad (\text{B15})$$

Similarly the normalization of the boundstate is determined by:

$$\sum_{j=1}^{l-1} \sinh^2 \kappa(j-l) = \frac{1}{2} \left[ (l-1) - \frac{\sinh \kappa(l-1) \cosh \kappa l}{\sinh \kappa} \right]. \quad (\text{B16})$$

The overlaps of band wavefunctions with and without the potential can be calculated similarly using:

$$\sum_{j=1}^{l-1} \sin k(j-l) \sin \tilde{k}(j-l) = \frac{\sin k(l-1) \sin \tilde{k} - \sin lk \sin(l-1)\tilde{k}}{2[\cos \tilde{k} - \cos k]}. \quad (\text{B17})$$

If  $k$  and  $\tilde{k}$  are allowed wave-vectors corresponding to potentials  $V_1$  and  $V_2$  respectively, then using Eq. (B4),

$$\sum_{j=1}^{l-1} \sin k(j-l) \sin \tilde{k}(j-l) = \frac{(V_2 - V_1) \sin k(l-1) \sin \tilde{k}(l-1)}{2t[\cos \tilde{k} - \cos k]}. \quad (\text{B18})$$

Thus we obtain the extremely useful result:

$$\langle \tilde{\Psi} | \Psi \rangle = \frac{(V_2 - V_1) C(\tilde{k}) C(k)}{\epsilon(k) - \epsilon(\tilde{k})}, \quad (\text{B19})$$

where  $\epsilon(k) = -2t \cos k$  is the band energy and

$$C(k) \equiv \frac{\sqrt{2} \sin k(l-1)}{\sqrt{(l-1) - \sin k(l-1) \cos kl / \sin k}}. \quad (\text{B20})$$

The corresponding result involving the boundstate follow immediately upon replacing  $\tilde{k}$  by  $i\kappa$ .  $\epsilon(\tilde{k})$  simply gets replaced by  $\epsilon_B \equiv -2t \cosh \kappa$  and  $C(\tilde{k})$  by

$$C_B \equiv \frac{\sqrt{2} \sinh \kappa(l-1)}{\sqrt{\sinh \kappa(l-1) \cosh \kappa l / \sinh \kappa - (l-1)}}. \quad (\text{B21})$$

To calculate the overlap of the  $V = 0$  groundstate with an arbitrary state with  $V \neq 0$ , we simply set  $V_1 = 0$  and  $V_2 = V$  in the above formula. This remarkably simple form for the overlaps of single particle wavefunctions leads to enormous simplification in the calculation of the overlap of the Bloch determinant multi-particle states, as shown in Section IV.

<sup>1</sup> Mahan G D 1967 Phys. Rev. **163** 612

<sup>2</sup> Nozières P and De Dominicis C T 1969 Phys. Rev. **178** 178

<sup>3</sup> Schotte K D and Schotte U 1969 Phys. Rev. **182** 479

<sup>4</sup> Hopfield J J 1969 Comments on Solid State Physics **II** 40

<sup>5</sup> Langreth D C 1970 Phys. Rev. **B 1** 471

<sup>6</sup> Combescot M and Nozières P 1971 J. Phys. (Fr.) **32** 913

<sup>7</sup> Pardee W J and Mahan G D 1973 Phys. Lett. **45A** 117

<sup>8</sup> Mahan G D 1975 Phys. Rev. **B 11** 4814

<sup>9</sup> Penn D R, Girvin S M, and Mahan G D 1981 Phys. Rev. **B 24** 6971

<sup>10</sup> Anderson P W 1967 Phys. Rev. Lett. **18** 1049; Phys. Rev. **164** 352

<sup>11</sup> Hawrylak P 1991 Phys.Rev. **B 44** 3821

<sup>12</sup> Affleck I and Ludwig A W W 1994 J.Phys. A: Math. Gen. **27** 5375

<sup>13</sup> Quin S, Fabrizio M, and Yu L 1996 Phys. Rev. B **54** 9854.

<sup>14</sup> Eder R and Sawatzky G (unpublished)

<sup>15</sup> Matveev K A and Larkin A I 1992 Phys. Rev. B **46** 15337.

<sup>16</sup> Geim A K *et al.* 1994 Phys. Rev. Lett. **72** 2061.

<sup>17</sup> Shields A J *et al.* 1995 Phys. Rev. B **51** 18049.

<sup>18</sup> Brown S A, Young J F, Brum J A, Hawrylak P and Wasilewski Z 1996 Phys. Rev. **54**, R11082.

<sup>19</sup> Affleck I 1996 Proc. Conf. "Advanced Quantum Field Theory (in memory of Claude Itzykson)", La Londe les Maures, France, Nucl. Phys. **B** to appear; hep-th/9611064.

<sup>20</sup> Pólya G and Szegő G 1945 Aufgaben und Lehrsätze aus der Analysis II, VII.Abschn.: §1, Nr.3 (Dover Publications, N.Y.)

<sup>21</sup> Landau L D and Lifshits E M Quantum Mechanics: Non-relativistic Theory: Oxford ; New York : Pergamon Press, 1989.

<sup>22</sup> Zagoskin A M (unpublished)